Journal of Structural Geology, Vol. 4, No. 2, pp. 161 to 176
Printed in Great Britain

0191-8141/82/020161-15 $03.00/0

Pencil structure and strain in weakly deformed mudstone and siltstone

IMANTS J. REKS and DAVID R. GRAY

Department of Geological Sciences, Virginia Polytechnic Institute & State University, Blacksburg, VA 24061, U.S.A.

(*Received* 3 *July* 1981; *accepted in revised form* 15 *February* 1982)

Abstract—Weakly deformed mudstone and siltstone (Middle Ordovician Knobs Formation) of the Appalachian Valley and Ridge Province, south-western Virginia, U.S.A. show strain-dependent transitions between bedding fissility, pencil structure and cleavage. Pencil structures are associated with a bulk inhomogeneous shortening deformation where minimum principal strain (Z) ranges between 9 and 26% shortening (assuming a plane strain and constant volume). Where strains are less, bedding fissility dominates. Pencil fragments are defined by intersecting fracture sets subparallel to the pre-existing bedding fissility and cleavage. Their long axes are both parallel to the bedding–cleavage intersection and to the inferred Y axis of the tectonic strain ellipsoid. Pencil development is considered to result from fracturing along both fabric anisotropies during weathering and post-tectonic stress relaxation. Pencils show variations in size and shape depending on lithology (grain size and composition), degree of initial clay preferred orientation, degree of cleavage development, type of cleavage, total bulk strain and degree of strain homogeneity. Their shape (l/w) however is a direct measure of total Y/Z strain since strain determinations from chlorite pressure-fringes on framboidal pyrite within the pencil fragments give

$$(Y/Z) = 0.913 + 0.019\ (l/w).$$

Pencil structure is therefore a potential strain marker in weakly deformed rocks.

INTRODUCTION

WEAKLY deformed mudrock commonly has a crude linear fabric which produces on weathering a mass of acutely terminated, elongate, polygonal fragments (Crook 1964). These elongate fragments have been referred to as pencil structure (Cloos 1957) or pencil cleavage (Graham 1978). They have been attributed to intersecting bedding fissility and cleavage (Cloos 1957, Crook 1964, Graham 1978, Engelder & Geiser 1979) or to superposition of tectonic strain on initial diagenetic compaction fabrics (Ramsay 1981). However, at present little is known firstly about the microstructure and morphology of the fabrics associated with pencil structures and, secondly about the factors which determine where, how and why pencils form. Also, if pencil structures are strain dependent (cf. Ramsay 1981), there is no clear understanding about their relations to total strain and their transition with other tectonic fabric elements. If these relations can be determined then these elongate, polygonal fragments are potential strain markers in weakly deformed mudrock.

This paper investigates pencil development in weakly deformed siltstone and mudstones in the Middle Ordovician Knobs Formation of the Southern Appalachian fold and thrust foreland (Valley and Ridge Province) in south-western Virginia, U.S.A. (Fig. 1). This portion of the belt is characterized by long, linear and arcuate, NE–SW trending thrust faults, some of which truncate regional anticlines and synclines. The rocks exhibit an incipient metamorphic fabric associated with deformation at temperatures between 250 and 350°C inferred from conodont colour alteration (Epstein *et al.* 1976). Analysis of pencil shapes, lithology and internal fabric are used to investigate the nature and origin of pencil structures. Three-dimensional strain analysis using pressure fringes adjacent to framboidal pyrites provides the basis for developing a relationship to total strain state.

PENCIL STRUCTURES

Outcrop morphology

Outcrops exhibiting well developed pencils are characterized by two sets of statistically-parallel fractures intersecting at high angles (Fig. 2a). A set of horizontal or gently dipping fractures, commonly 4–12 mm apart, is parallel to a bedding-parallel fabric. A second approximately vertical fracture set is parallel to a cleavage related fabric. Fracture spacing ranges from 2 to 10 mm. Fractures appear planar, forming continuous to discontinuous traces in sections perpendicular to bedding. They are commonly refracted as they pass from one lithology into another. Fracture traces in the bedding plane form an anastomosing network dividing the rock into elongate, acutely terminated fragments (Fig. 2b). Fragments vary in size, ranging from 20 to 140 mm in length, and are elongate parallel to cleavage and local fold axes. Weathered out blocks commonly splinter into smaller pencil-like fragments (Fig. 2c).

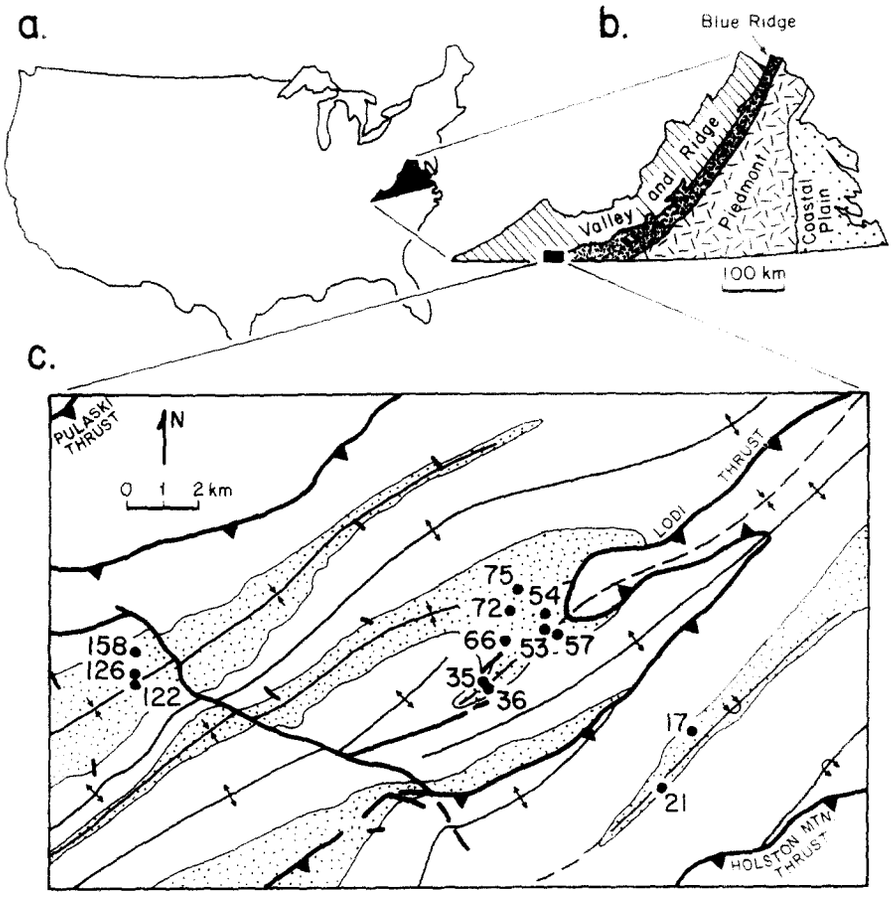

Fig. 1. Location maps (a) continental U.S.A. showing Virginia (stippled), (b) geological provinces of Virginia, (c) geologic map of study area showing outcrop pattern of the Knobs Formation, thrust-fault and fold axial surface traces. Sample localities are shown (see Appendices I and II for description).

Pencils occur in shales, rhythmically banded mudstones and siltstones. They are not developed in interbedded lithic sandstones. Pencils are best developed in areas where strata are gently warped and have moderate dips. In areas of intense folding and faulting, pencils are absent and a well developed cleavage is present.

Pencil shape

Pencils in outcrop show variations in size, shape and termination of fragments (Figs. 3a–c). These variations produce a complete spectrum of pencil types. In profile, pencil shape ranges from square or rectangular to rhom-

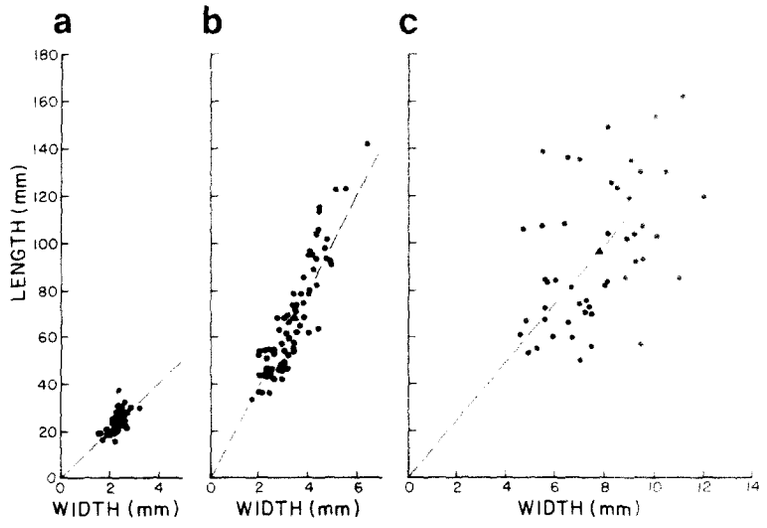

Fig. 4. Pencil length (l) vs width (w) plots. The dashed line represents shape factor line and corresponds to the pencil l/w ratio. (a) Point distribution; locality 57 ($l/w = 10.39$). (b) Linear distribution; locality 21 ($l/w = 19.83$). (c) Diffuse linear distribution; locality 72 ($l/w = 12.73$).

bic, depending on bedding–cleavage angle and spacing of bedding fissility and cleavage–parallel fractures. Pencil shape can be specified by a shape factor ratio (l/w) determined by the length (l) and width (w) of the fragments measured in the bedding plane. Pencil thickness (t), in this case dependent on bedding fissility spacing, was not included. Width (w) corresponds to the spacing between cleavage–parallel fractures.

Although pencils appear to show variability in outcrop, they show consistent relationships on length vs width plots (Figs. 4 and 5). Shape factor (l/w) values from all outcrops analysed range from a low of approximately 9 (short and stubby shapes) to a high of about 25 (long and slender shapes) (Fig. 4). Pencils with higher or lower values are not developed. The shape factor line is a line with negative slope connecting the origin with the mean of each length vs width distribution. Three distinct types of distributions occur, including point clustering (Fig. 4a), linear groupings (Fig. 4b) and diffuse linear groupings (Fig. 4c). The amount of scatter on these graphs indicates the degree of uniformity of pencil size and shape for each sample of pencils. Low scatter, such as a point distribution, reflects uniform size and shape, whereas a linear grouping indicates uniform shape but varying pencil size. Diffuse linear groupings show the most irregularity, both in size and shape, for pencil samples.

Degree of anastomosing of cleavage traces is another factor affecting pencil shape. Since the positions where undulating and anastomosing cleavages coalesce correspond to the terminations of pencils (Fig. 3), the angle (θ) between coalescing cleavage traces measured in planes parallel to bedding, is a function of their degree of anastomosing. Slightly undulating cleavage traces have lower θ values than highly anastomosing traces. This angle also varies with pencil shape (Fig. 6). The lowest angles correspond to the highest shape factors. Highly anastomosing cleavages, therefore, produce pencils with low shape factors, whereas gently undulating cleavages give pencils with high shape factors. Shape factor values and angles θ can also be affected by cross-cutting joint sets which reduce the pencil length. Pencils with flat terminations due to cross-fracturing give anomalous values and were, therefore, not included in the analysis.

Pencil shape also varies with change in bedding/cleavage angle ($\widehat{S_0S_1}$). Highest shape factors are associated with bedding/cleavage angles close to 90° (Fig. 7). The graphed relation suggest that pencil shape is varying across the regional folds, since bedding/cleavage angle reflects structural position in folded terrains.

Internal pencil fabric: cleavage microstructure and interpretation

A spaced cleavage, morphologically ranging from a rough to intermediate variety (Powell 1979) occurs in shales, mudstones and siltstones associated with pencil structures. In outcrop, the fissility at high angles to bedding is a visible expression of the cleavage microstructure (Figs. 8a & b). The domainal microfabric is characterized by thin cleavage lamellae (1–5 μm wide) alternating with thicker intercleavage zones (5–40 μwide) where phyllosilicates are oriented at high angles to the cleavage lamellae and define a weak sedimentary bedding fabric (Fig. 8c).

Cleavage domains consist of thin discrete selvages

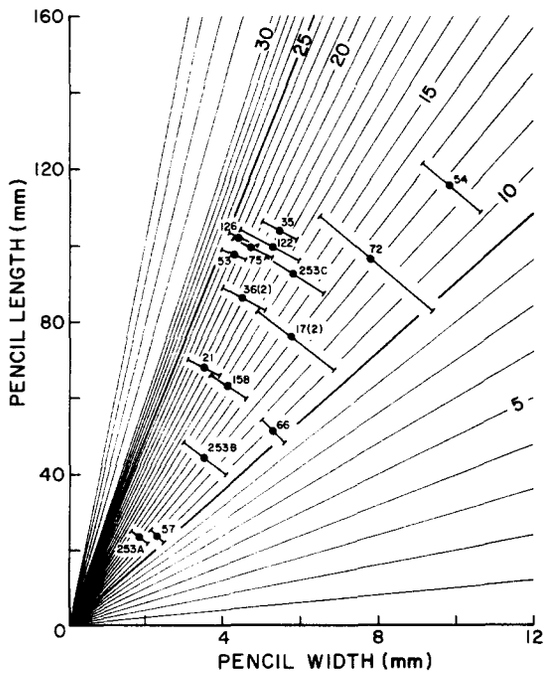

Fig. 5. Pencil shape factor graph. Points represent means of 35–100 measurements of pencils at sixteen localities (see Appendices I and II). Error bars indicate standard deviations.

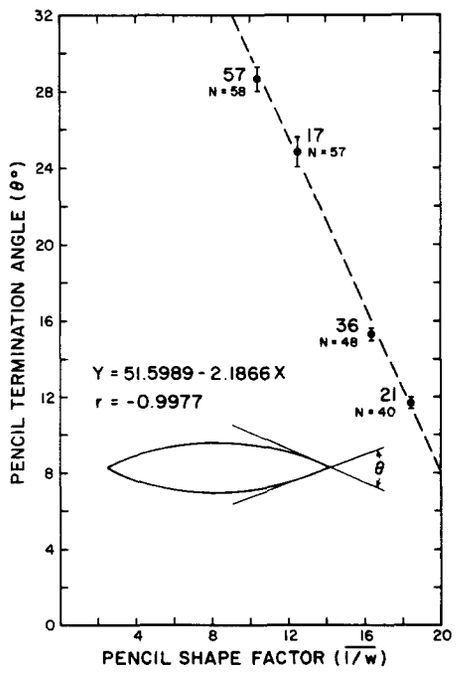

Fig. 6. Pencil shape factor (l/w) vs pencil termination angle ($\bar{\theta}$). Points represent means of 40–60 measurements from four localities (see Appendices I and II). Standard deviations indicated by error bars. Line of best fit and correlation (r) are given.

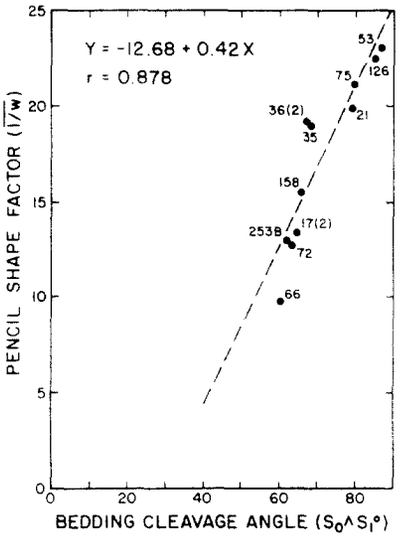

Fig. 7. Plot of pencil shape factor ($\overline{l/w}$) vs bedding–cleavage angle (S_0S_1). Points represent means from 11 localities (see Appendices I and II). Line of best fit and correlation coefficient (r) are given.

which truncate the pre-existing bedding fabric. They are defined by closely packed clays which have a moderate to strong dimensional preferred orientation parallel to the domain boundaries (Fig. 8c). Detrital quartz and chlorite grains adjacent to cleavage are truncated, exhibiting sutured boundaries while grains between the lamellae remain relatively equant (Fig. 8d). Quartz grains within the lamellae are rare but where present have high axial ratios parallel to the cleavage. Also bedding and pre-cleavage quartz and calcite veins are offset along the cleavage (Fig. 8d). These features suggest that cleavage lamellae are pressure-solution seams (also see: Stringer & Lajtai 1979) along which chlorite and minor amounts of quartz and calcite have been dissolved, leaving a concentration of less mobile clays. Neocrystallization of phyllosilicates is also suggested by incipient herringbone patterns of small, clear micas (cf. Holeywell & Tullis 1975) and chlorite growth in pressure fringes on framboidal pyrite.

Morphology of the cleavage microfabric varies with the intensity of cleavage development. Fabric in pencils with weak cleavage is a rough disjunctive variety (Powell 1979). The cleavage domains consist of short discontinuous and irregular seams that envelop detrital grains (Figs. 9a & b). In pencils where cleavage is better developed, the short discontinuous lamellae join to form somewhat more planar, continuous seams (Figs. 9c & d). This morphology is transitional between rough and smooth types (Powell 1979). In regions where pencils are absent, cleavage approaches a smooth disjunctive type giving rise to an incipient metamorphic texture. Intensity of cleavage development and type of cleavage also varies through and across individual pencils. Centres of pencils show weaker development of cleavage to terminations of pencils, where cleavage spacing is significantly lower.

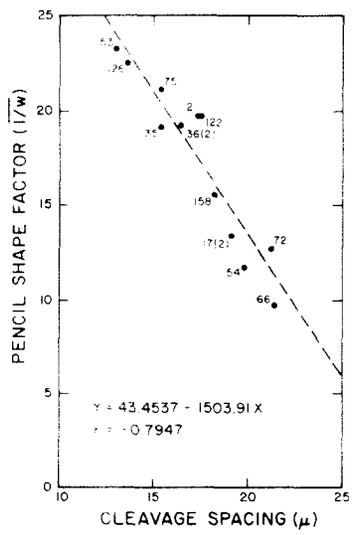

Fig. 10. Graph of pencil shape factor (l/w) vs cleavage spacing (μ) from pencil centres. Points represent means of 50 spacing measurements at seven localities (see Appendix I). Line of best fit and correlation coefficient (r) are given.

RELATIONS OF PENCILS TO STRAIN

At present little is known about pencils in terms of strain state. Where strain has been determined (Graham 1978, Ramsay 1981) pencils are associated with unaxial prolate ellipsoids ($k = \infty$) and are elongate parallel to the total maximum principal extension direction (X). Long axes of pencils in red mudstones of the Cambrian Dundas Group near Zeehan, Tasmania are also statistically parallel to the extension direction defined by reduction spots ($k = 2.18$) (Reks 1981). Existing data, therefore, indicates that pencil structure is a strain-related phenomenon. This section examines pencils and strain in the Knobs Formation and attempts to derive a relation between them.

Cleavage spacing and pencil shape

A stronger fabric anisotropy is developed in pencils with high shape factors (compare Figs. 9a & b with Figs. 9c & d). Cleavage becomes more continuous, anastomosing and better developed with increasing shape factor values. This is supported by cleavage-spacing data from the pencil samples (Fig. 10). There is a progressive decrease in cleavage spacing with increasing shape factor. Although the relationship between the development of slaty cleavage and total strain is still problematical, regional studies (Siddans 1977, Graham 1978, Wood & Oertel 1980) indicate that the degree of perfection of slaty cleavage increases with increasing strain. It can therefore be assumed that the degree of cleavage intensity (i.e. continuity, thickness and spacing of lamellae) is an approximate measure of bulk rock strain.

Pencil shape within the Knobs Formation must, therefore, be strain dependent since cleavage spacing progressively decreases with higher shape factor (Fig. 10). This implies that pencils with high shape factors develop in rocks with higher bulk strain than those containing pencils with lower shape factors. Variations in quartz grain size are also associated with this relation-

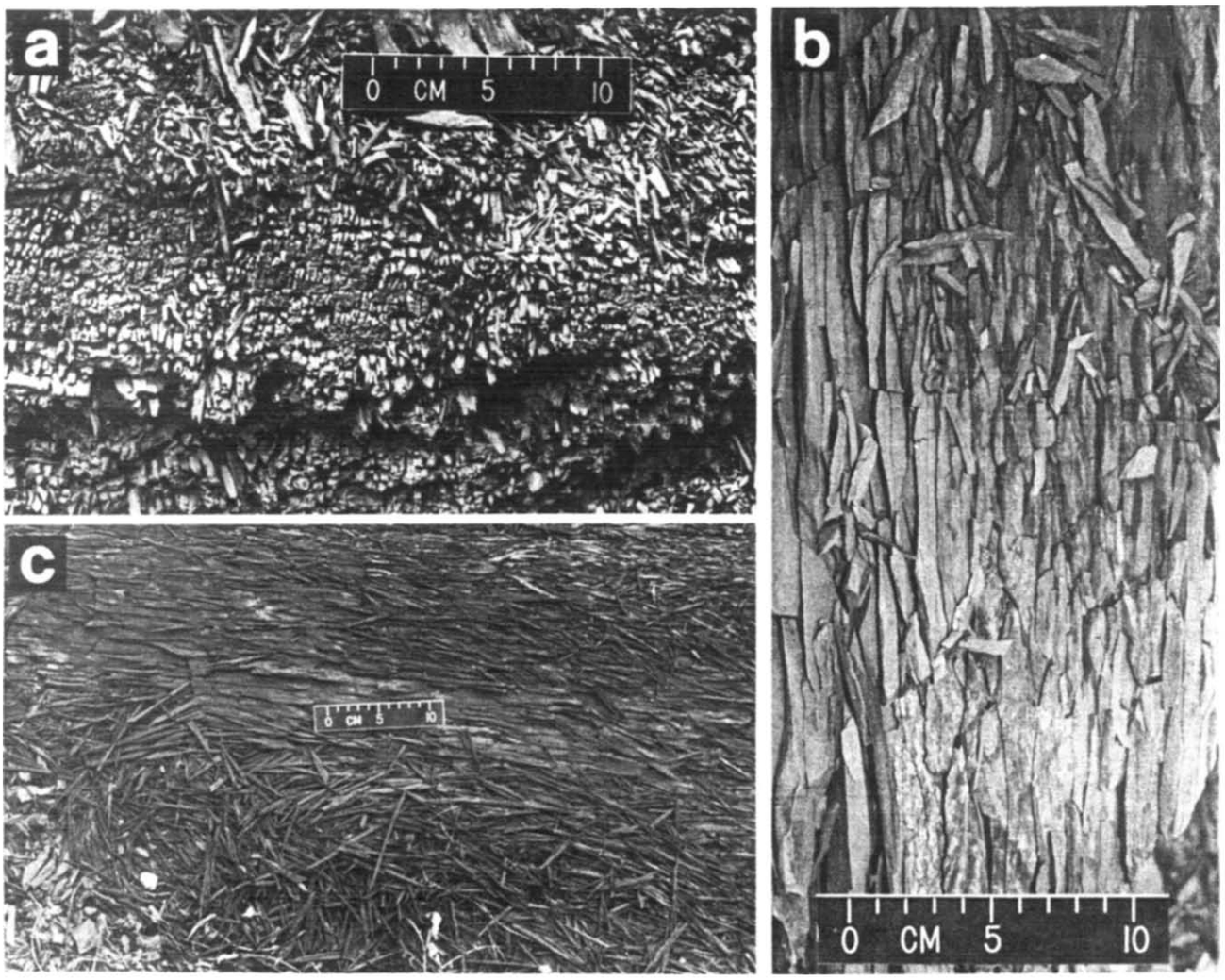

Fig. 2. Outcrop morphology of pencils in the Knobs Formation. (a) Photograph perpendicular to bedding and cleavage showing two sets of intersecting fractures (locality 158). Bedding is horizontal and cleavage is vertical. (b) Bedding surface showing pencil development, locality 17(2). (c) Outcrop showing weathered out pencils, locality 21.

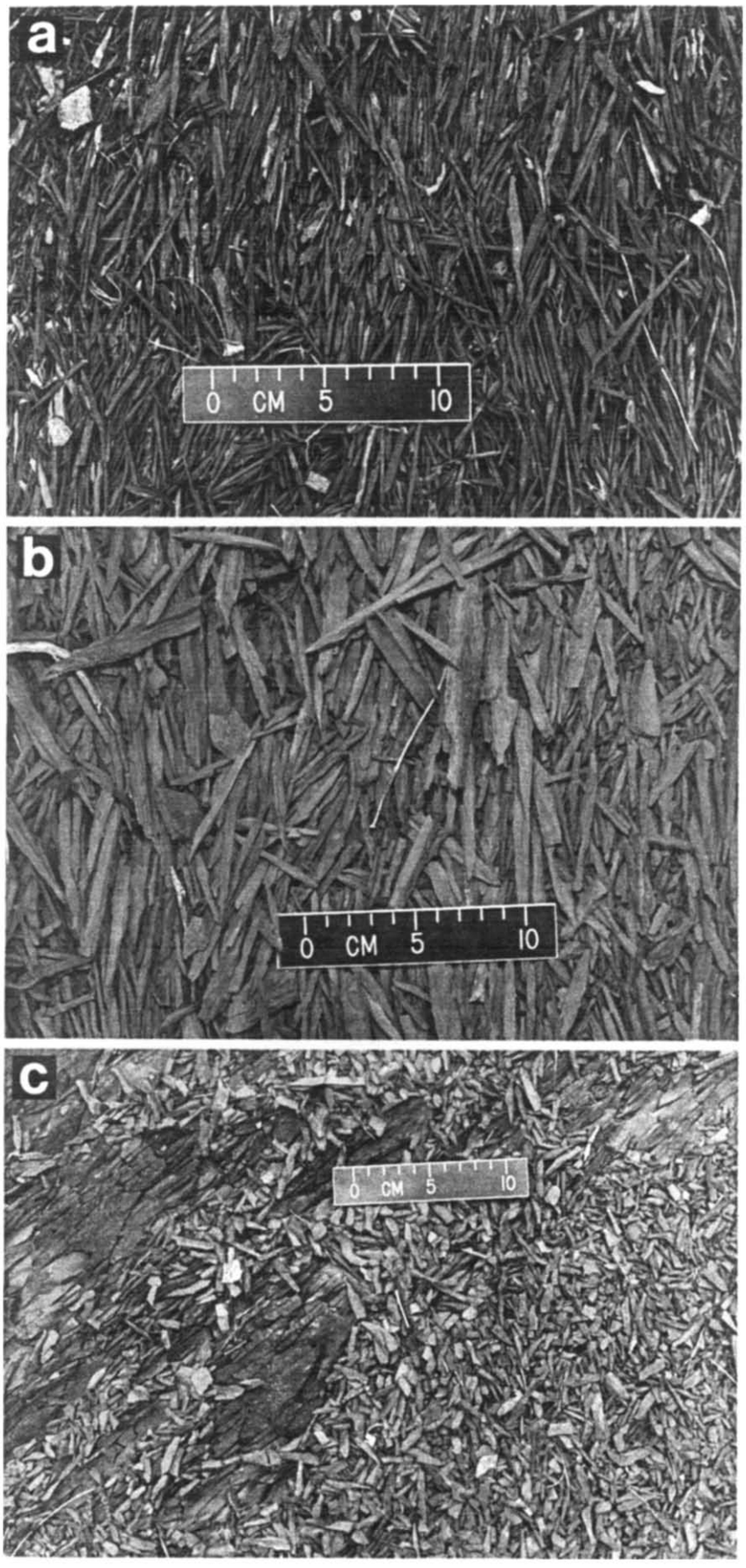

Fig. 3. Variations in pencil sizes and shapes. (a) Long and slender fragments in black shales (locality 21, $l/w = 19.83$, $\bar{\theta} = 11.69°$). (b) Long stubby fragments in mudstones (locality 17(2), $l/w = 13.42$, $\bar{\theta} = 24.8°$). (c) Short and stubby fragments in mudstones (locality 57, $l/w = 10.39$, $\bar{\theta} = 28.58°$) (for locations see Fig. 1).

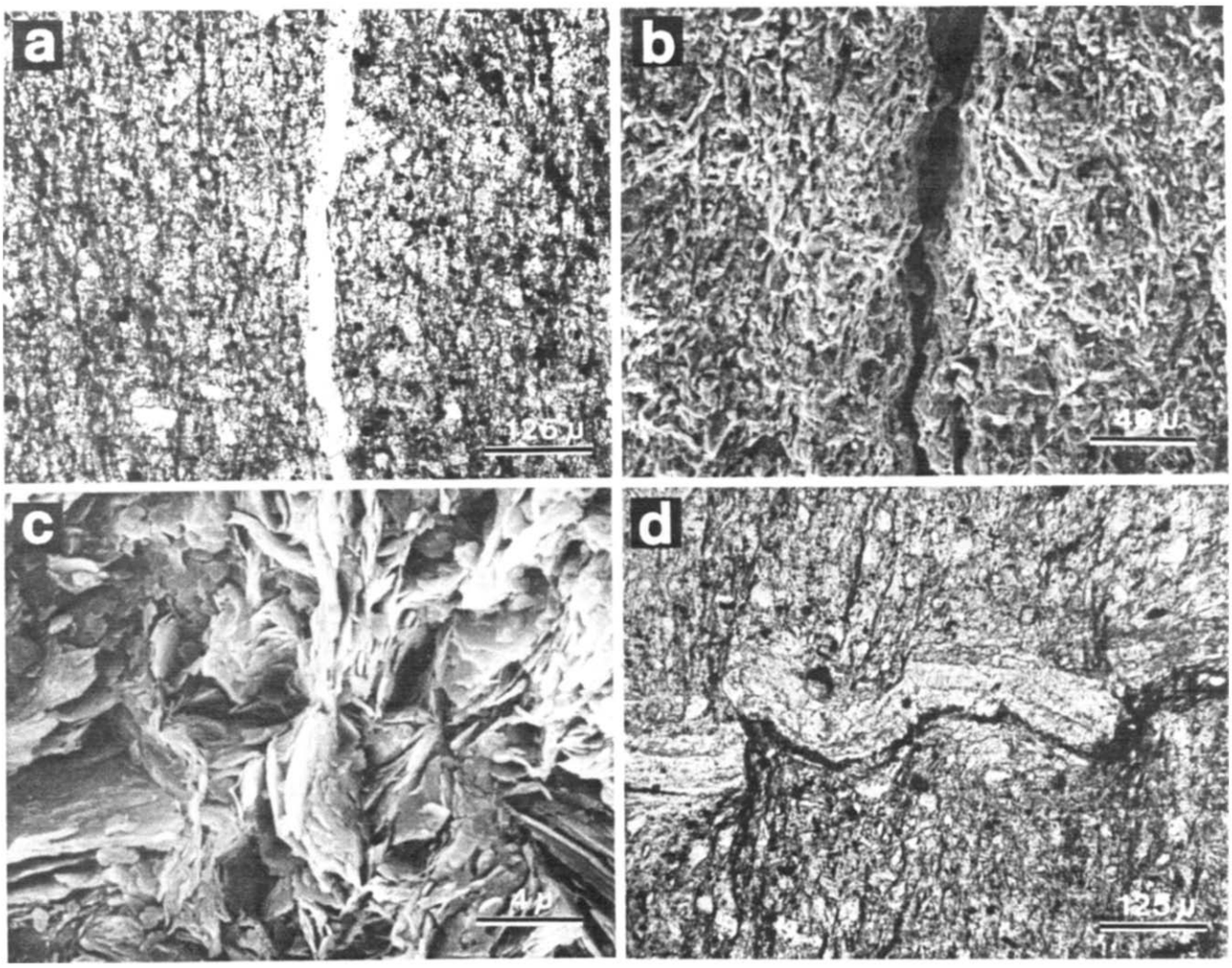

Fig. 8. Cleavage microstructure of pencil fragments from locality 17(2). (a) Photomicrograph (PPL) of fracture parallel to the cleavage fabric. (b) SEM micrograph of fracture parallel to cleavage fabric. (c) SEM micrograph showing cleavage lamellae defined by parallel clay platelets (vertical) truncating preexisting bedding fabric (horizontal). (d) Photomicrograph (PPL) showing calcite vein parallel to bedding offset along cleavage seams.

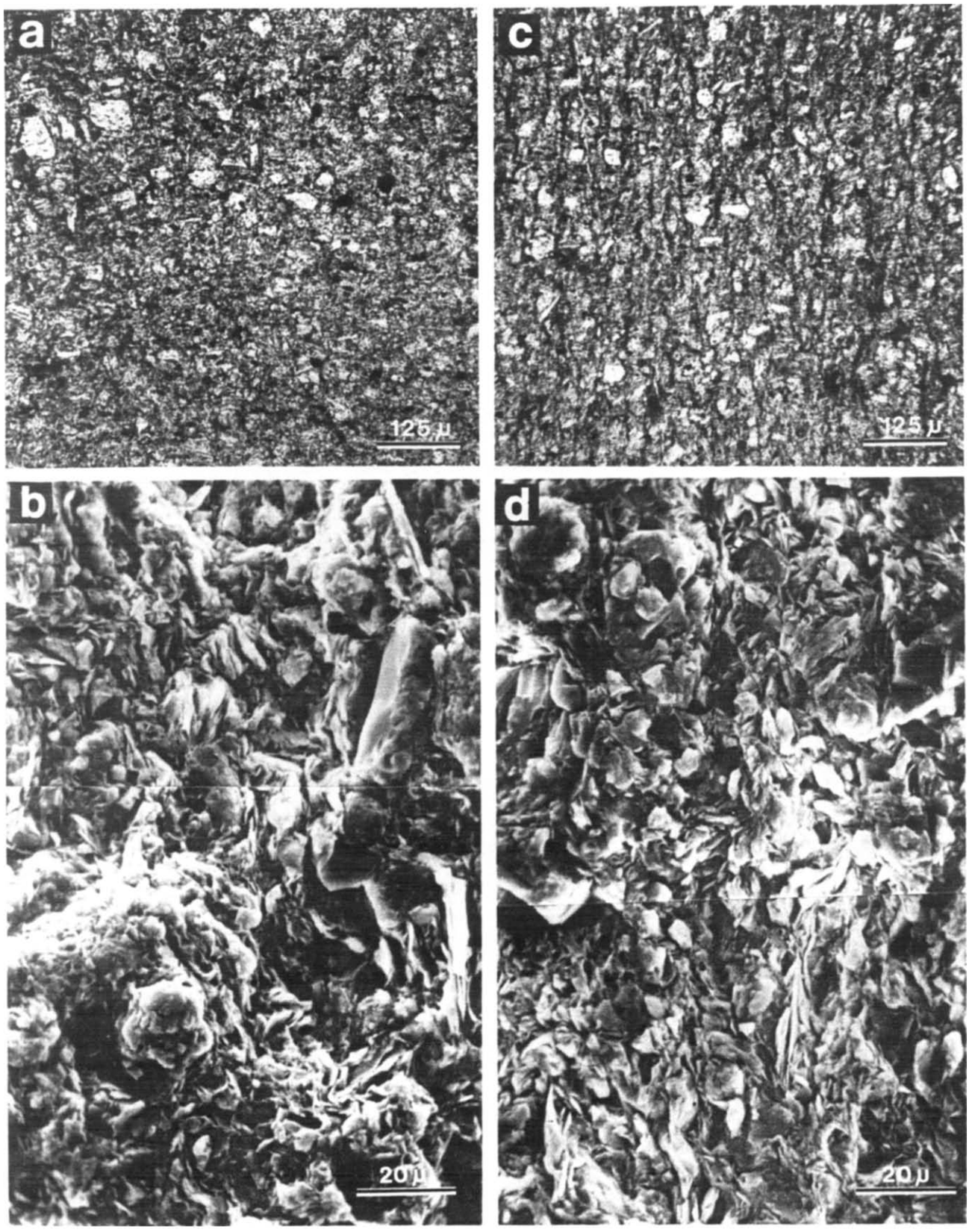

Fig. 9. Variations in cleavage microfabric associated with changes in pencil shape factor (l/w). (a) Photomicrograph (PPL) and accompanying SEM micrograph (b) of pencil fabric in sections perpendicular to cleavage and bedding. Bedding is horizontal and cleavage is vertical (locality 66: $l/w = 9.76$). (c) Photomicrograph (PPL) and accompanying SEM micrograph (d) of pencil fabric in sections perpendicular to cleavage and bedding. Bedding is horizontal and cleavage is vertical (locality 53: $l/w = 23.09$).

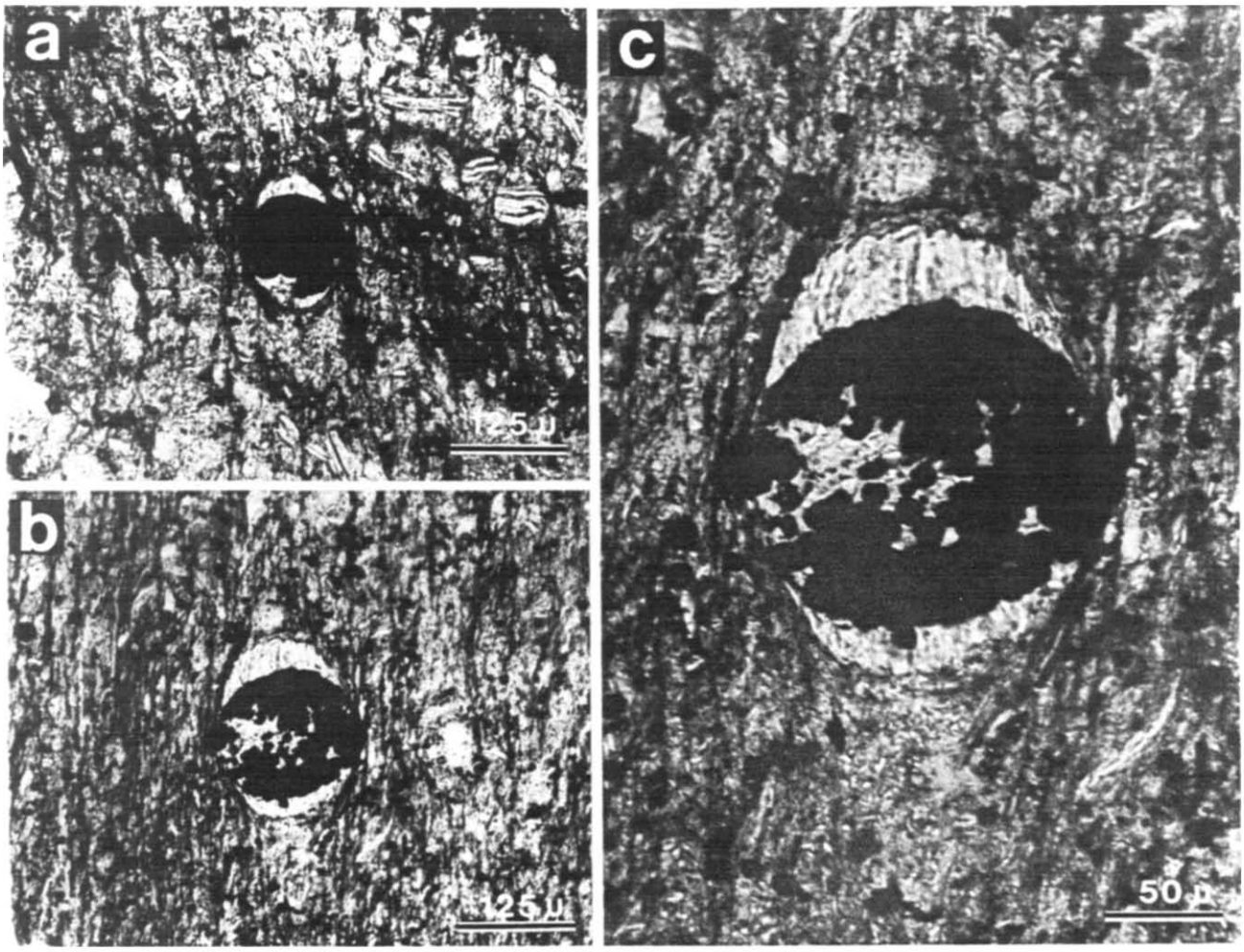

Fig. 12. Photomicrographs (PPL) of chlorite pressure fringes on framboidal pyrite in (a) pencil fragment at locality 53 (l/w) = 23.09, Y/Z = 1.35), (b) cleaved mudstone without pencil structure at locality 36(1) (Y/Z = 1.67) and (c) an enlargement of (b).

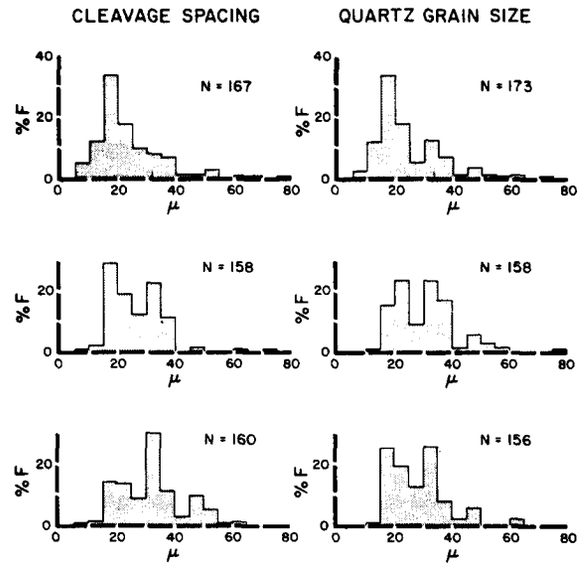

Fig. 11. Cumulative frequency, histograms showing cleavage spacing and quartz grain size (width) distributions. (a) Locality 53 (l/w = 23.09). (b) Locality 35 (l/w = 19.14). (c) Locality 66 (l/w = 9.76). N is the number of measurements.

ship (Fig. 11). The 33–35 μm peak which is prominent at the lower shape factors is substantially reduced at higher shape factors while the 15–20 μm peak is enlarged. Accentuation of the 15–20 μm peak results from reduction of the 30–35 μm size quartz grains by pressure-solution with increasing development of cleavage.

Incremental strain history and total strain

Incremental strain histories can be determined by using syntectonic crystal-fibres in pressure fringes adjacent to pyrite concretions (Durney & Ramsay 1973, Wickham 1973, Gray & Durney 1979). Finite strains can then be calculated from the displacement paths preserved by the fibres. It is assumed that pressure fringe growth begins when ductile extension commences in the matrix.

Pressure fringes adjacent to framboidal pyrites in shales and mudstones of the Knobs Formation consist of straight fibres of chlorite (Fig. 12). The fibres show characteristics of antitaxial growth (cf. Durney & Ramsay 1973, pp. 82–83). The association of pressure-fringes with pencil development provides an opportunity to derive a unique relationship between pencil shape and total strain.

Method of analysis. Values of principal elongation (e_1) were determined according to the "Pyrite Method" (Durney & Ramsay 1973, p. 92). The method assumes that fibres are parallel to the principal extensions in the rock and that no relative body rotation has taken place. Calculated strains therefore record only the internal deformation of the rock. The incremental extension is given by:

$$\text{Incremental } e_{l_n} = \frac{\text{chord length}_n}{\sum_{0}^{n-1} \text{chord length } i \cos\theta_i + \text{pyrite radius}},$$

where θ_i is the angle between the ith chord and the nth chord. Since fibres in these fringes are straight the equation reduces to:

$$e_1 = l_n/l_0 = \frac{\text{fibre length}}{\text{pyrite radius}}.$$

Pressure fringes were examined along three mutually perpendicular directions in sections corresponding approximately to XZ, YZ and XY planes of finite strain (X, Y and Z are the maximum, intermediate and minimum elongation directions, respectively). Section directions were selected by consideration that cleavage was parallel to XY and fibres in sections parallel to

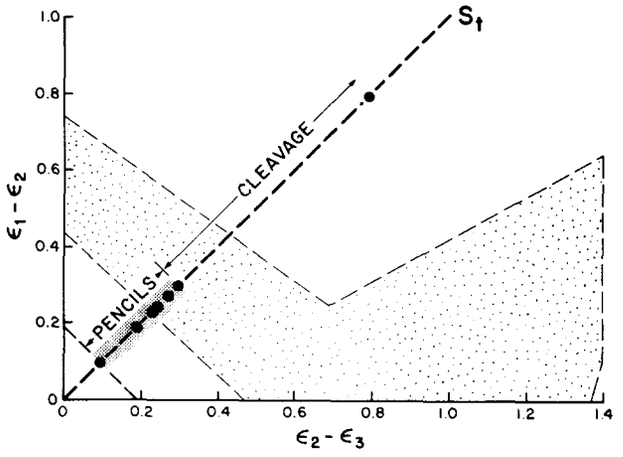

Fig. 13. Logarithmic Flinn diagram with total tectonic strain data (calculated from pressure fringes in mudstones and siltstones) from the Knobs Formation. Sample localities in order of increasing strain are 66, 158, 35, 36(2), 21, 53 and 36(1). Stippled area shows progressive deformation path for slates with both pencil structure and cleavage, Alpes-Maritimes, France (see Graham 1978, fig. 15). Minimum initial compaction (assuming superposition of plane strain on compaction) for the Knobs Formation mudstones is approximately 18%; calculated from $\ln(1 + \Delta_{ii}) = (\varepsilon_1 - \varepsilon_2) - (\varepsilon_2 - \varepsilon_3)$ (Ramsay & Wood 1973, eqn 8).

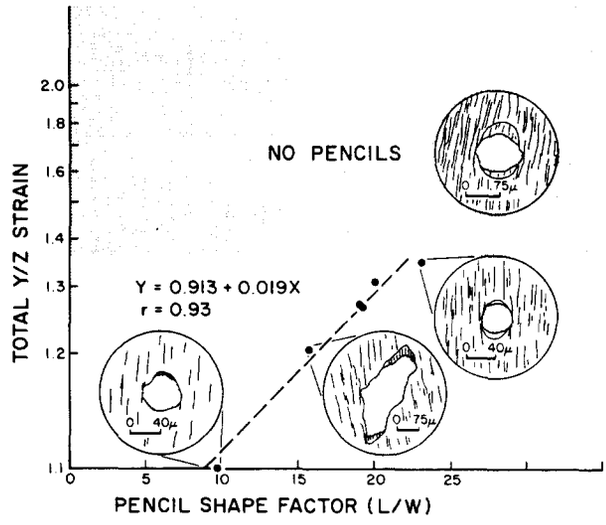

Fig. 14. Semi-log graph of Y/Z axial ratio of finite strain ellipsoid vs pencil shape factor (l/w). Stippled area represents values associated with well developed cleavage. Representative pressure fringes are shown. Sample localities in order of increasing strain are 66, 158, 35, 36(2), 21 and 53. Line of best fit and correlation coefficient (r) are given.

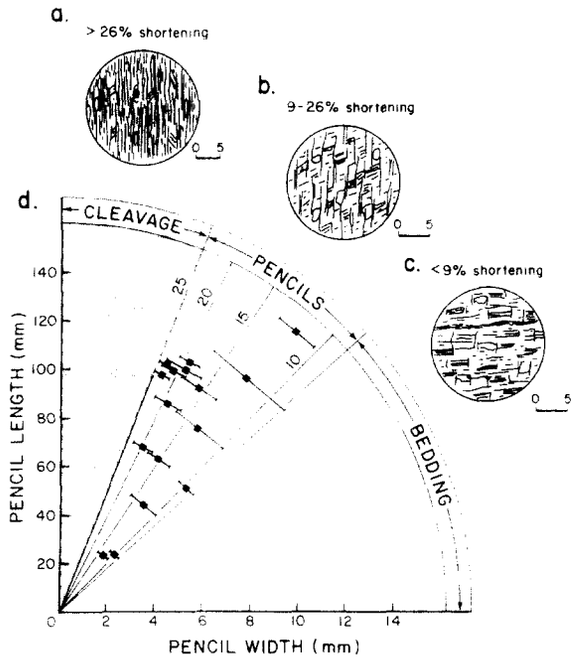

Fig. 15. Diagram showing variations in microfabric associated with progressive deformation. (a) Diagrammatic sketch of cleavage microfabric at strains greater than 26% shortening. (b) Diagrammatic sketch of internal pencil fabric at strains between 9 and 26% shortening. (c) Diagrammatic sketch of bedding fabric with incipient cleavage at strains less than 9% shortening. (d) Pencil length (l) vs width (w) graph showing domainal distribution of each fabric.

cleavage designated X. The analysis enabled determination of the total strain ellipsoid. Pressure fringes are absent from all YZ sections, indicating no extension parallel to Y (i.e. $1 + e_2 = 1$). Although elongation in X is recorded by the fibres, minimum elongation (Z) cannot be determined from the pressure fringes. The simplest assumption is designation of $1 + e_3(Z)$ as the reciprocal of $1 + e_1(X)$, that is plane strain with no volume change.

Strain state of pencils. Since XZ sections show pressure fringes with straight fibres the deformation sequence must have been coaxial. This requires coincidence between, and constant orientation of, principal axes of both incremental and progressive strain throughout the deformation. Extension directions determined from the fibres are parallel to the local cleavage traces in XZ sections. Designation of $1 + e_3$ as $1/(1 + e_1)$ (see above), and with $1 + e_2 = 1$ dictates a plane strain deformation sequence (Fig. 13). This assumption must be correct to a first order approximation since mudrock/siltstone microfabrics are weak $L \simeq S$ tectonites. Total strains associated with pencils are low and range from 1.10:1:0.91 to 1.35:1:0.74.

Pencil shape variations are influenced by total YZ strain (Fig. 14). (Since pencil shape is defined in the YZ plane when bedding and cleavage are approximately perpendicular, it was compared to the YZ section of the total strain ellipsoid.) Highest strains correspond with

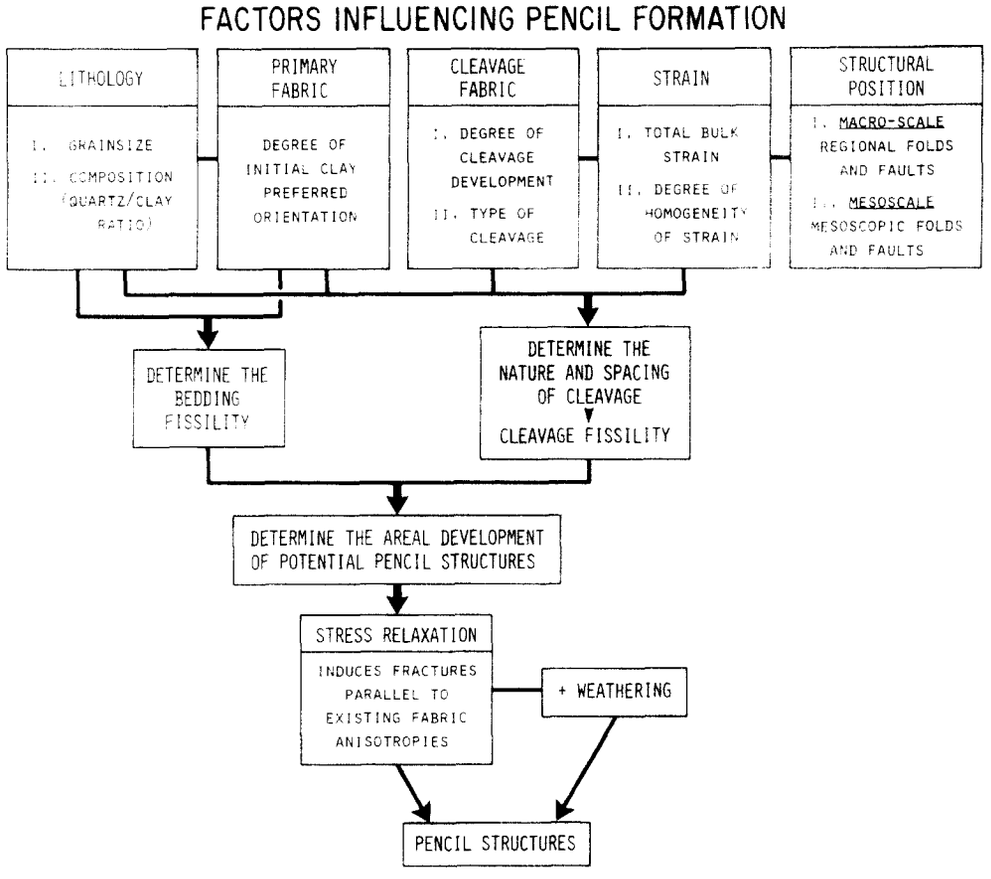

Fig. 16. Flow diagram showing interrelations between various parameters affecting pencil development.

the highest pencil shape factors. The derived relation

$$(Y/Z) = 0.913 + 0.19\,(l/w)$$

is unique for the mudstones and siltstones of the Knobs Formation. Strain values for localities where pencils are not developed are also plotted (stippled area). It is important to note that pencil development is restricted to a narrow window of tectonic strain values ($1.1 \leq Y/Z \leq 1.35$). Where strains are greater than $Y/Z = 1.35$ (26% shortening), pencils are not developed. Similarly where strains are less than $Y/Z = 1.1$ (9% shortening), pencils are absent.

Since these pressure-fringes do not record compactional strains due to volume loss (Δ), strains determined from the fibres only represent the tectonic strain and not the total bulk strain of the rock. Coaxial superposition of tectonic plane strain and compactional strain produces a complex deformation path, where total strain moves from the flattening to the constriction field and back to the flattening field during deformation (cf. Sanderson 1976, fig. 3, Graham 1978, fig. 15). Pencil structures are associated with total strain in the construction field for this deformation path (see Graham 1978, fig. 14, Ramsay 1981). It is possible that pencils in the Knobs Formation, although defined by intersection of two planar fabric anisotropies, are associated with a total bulk strain in the constriction field. Boundary conditions of the deformation sequence discussed previously would correspond to Case 1 of Sanderson (1976).

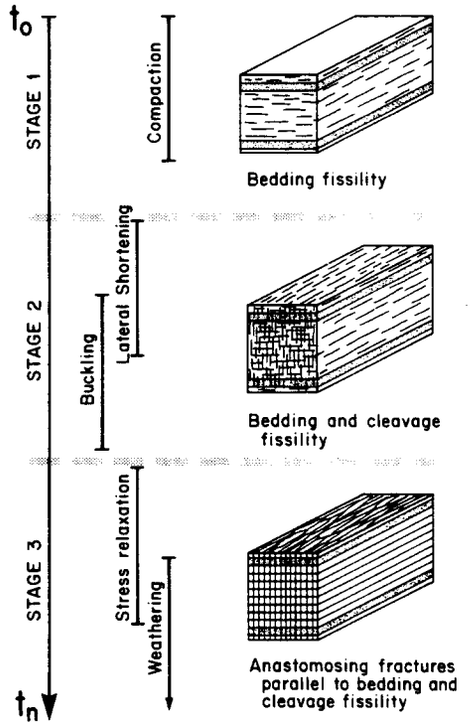

Fig. 17. Schematic diagram illustrating the three main stages in pencil formation and their respective fabrics. Linear time sequence (t) shows the dominant processes affecting the rock during each stage.

DISCUSSION: FORMATION AND INTERRELATIONS BETWEEN PENCIL STRUCTURE AND CLEAVAGE

Field and microfabric observations (see previous section) indicate that formation of pencils in weakly deformed siltstones and mudstones of the Middle Ordovician Knobs Formation requires the presence of two independent anisotropy directions. These are a bedding fabric and a cleavage fabric. The bedding fabric is defined by elongate chlorites oriented with their (001) cleavage planes parallel to bedding, whereas cleavage fabric is defined by a dimensional-preferred orientation of smaller phyllosilicate minerals. Progressive variations in mudstone/siltstone microfabrics are associated with changes in pencil shape. Increased degree of clay preferred orientation, lengthened cleavage traces, decreased cleavage spacing and lower degrees of anastomosing, characterize pencils with high length to width ratios. These changes, as well as changes in pencil shape and intensity of development, are clearly strain dependent (Fig. 15). At strains below a certain critical value (<9% shortening), cleavage development is incipient (Fig. 15c). Since bedding remains the dominant plane of anisotropy, pencil development is inhibited. At strains greater than 26% shortening, cleavage is well developed (Fig. 15a). Although traces of bedding are still present, it has largely been obliterated by the new tectonic fabric. Unless a second equally pervasive tectonic fabric is superimposed, pencils cannot develop. Pencil development in the Knobs Formation is therefore restricted to a window of strain values which represents a balance between two independent fabrics where neither totally dominates (Fig. 15b). Pencil structure is, therefore, a strain dependent fabric element which is transitional between bedding fissility and cleavage. It only occurs in weakly deformed and, therefore, poorly cleaved rocks.

The actual development of pencil structure is, however, dependent on the complex interaction of several variables, including lithology, primary fabric, cleavage fabric, strain, structural position, stress relaxation and weathering (Fig. 16). Lithology, reflected by grain size and composition, and the degree of initial clay preferred orientation determine the intensity of bedding fissility. Variations in lithology not only restrict the development but influence the pencil shapes. Pencils are developed in siltstones and mudstones but are absent from sandstones. Different size fragments with the same shape factor (l/w ratio) result from slight differences in lithology. Rocks with an initially random sedimentary fabric cannot develop pencils because they lack the necessary fissility parallel to bedding. The cleavage fabric, dependent on the operative deformation mechanisms, and the magnitude and homogeneity of strain which is in part dependent on structural position, determine the intensity of cleavage fissility. With approximately equal development of bedding and cleavage fissilities the final stage in pencil development is considered to be an interaction of stress relaxation and weathering (Fig. 16). Stress relaxation, caused by the removal of overburden or tectonic confining pressures (Friedman 1972,

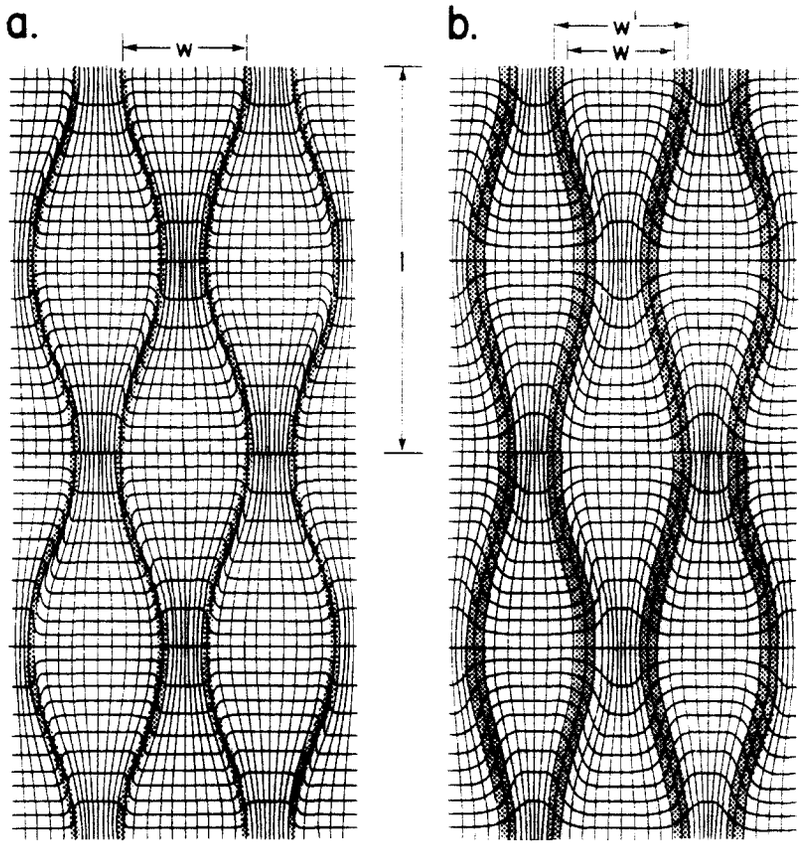

Fig. 18. Idealized patterns of anastomosing foliations and strain distributions associated with a progressive bulk homogeneous shortening deformation (modified from Bell 1981, fig. 6). (a) Inhomogeneous strain distribution. Note the narrow zones of high strain (cleavage). l and w correspond to the length and width of potential pencil structure. (b) More homogeneous strain distribution. Note the wider zones of high strain (cleavage). l, w and w' correspond to length, minimum width and maximum width, respectively, of potential pencil structure.

Engelder & Sbar 1977, Holzhausen & Johnson 1979), produces strain-induced fractures parallel to the pre-existing fabric anisotropy directions. These are enhanced by local weathering processes. The described interrelations between conditions, fabrics and processes necessary for pencil formation are represented diagrammatically in Fig. 17. Stage I fabrics are due to deposition and compaction. Stage II is related to layer parallel shortening and low amplitude, open folding and Stage III is associated with uplift and exposure at the Earth's surface.

Another important aspect of pencil formation is the variation in shape. Although strain related, there is no clear explanation as to why the cleavage anastomoses, particularly when it develops subparallel to the XY principal plane of strain (Fig. 12). Anastomosing cleavage traces on bedding surfaces may indicate that cleavage formed by progressive bulk inhomogeneous shortening (Bell 1981). Traces must anastomose if the foliation is to remain planar on the average and reflect variations in strain. If constant volume is maintained, then local increase in strain will be accommodated by a local decrease in an adjacent region, producing the geometry shown in Fig. 18 (see Bell 1981, fig. 6). Geometrical constraints of the model require that (1) foliations anastomose less and tend toward planarity with increasing strain (i.e. pencils would develop higher length/width ratios), (2) higher local strains exist where foliations coalesce and (3) foliation thickness is dependent on the degree of strain inhomogeneity (Fig. 18). (1) and (2) have been documented for pencil structure in the Knobs Formation, whereas (3) provides an explanation for the scatter shown by diffuse linear pencil shape distributions (Fig. 4c). As strain is more inhomogeneously distributed, the anastomosing zones of high strain become progressively smaller, concentrating the strain along thin discrete traces (Fig. 18a). in terms of pencil shape, where strain is inhomogeneous, the anastomosing zones of high strain (cleavage) are narrow and well defined. Later fracturing will, therefore, occur along these thin, well defined planes forming uniformly shaped fragments, shown by distributions in Figs. 4(a) & (b). Where strain is more homogeneously distributed, the zones of high strain (cleavage) become wider and more diffuse (Fig. 18b). Later fracturing can occur anywhere along the larger zone and pencil shape is therefore potentially more variable, as shown by the distribution in Fig. 4(c).

Although the geometric models of Bell (1981) are for constant volume, pressure-solution accompanied by volume loss, will only enhance relations (1) and (2) dictated by the model. Volume loss along developing cleavages (Fig. 18, stippled zones) would cause further reduction in the termination angle (θ) and reduce the

degree of cleavage anastomosing. We, therefore, suggest that pencil structure in the Knobs Formation is probably due to a weak, bulk inhomogeneous shortening deformation. As the deformation progresses however strain becomes more homogeneously distributed and a strong cleavage fabric develops.

A final aspect important to pencil development is the strain state and associated fabric type. Pencils in the Knobs Formation are defined by the intersection of a primary fabric (bedding) with a tectonic fabric (cleavage). Pressure fringes record approximate plane strain with the principal tectonic elongation direction (X) vertical in the plane of cleavage. As a result both the intersection lineation and pencil elongation are subparallel to local fold axes, but not to the principal tectonic elongation direction (X). Pencil structures can also develop in deformed rock associated with a constrictional strain state and show no distinct fabric anisotropies in outcrop (e.g. Cretaceous marls in the Diablerets and Wildhorn nappes Switzerland: Ramsay 1981; Cambrian Dundas Group, Zeehan, Tasmania; Reks 1981). These pencils are elongate parallel to the X direction of total strain. We suggest, therefore, that pencil structures can either develop from (1) intersection of two independent fabric anisotropies or (2) as a linear fabric-element in constrictional strain. In both cases pencils will be oriented perpendicular to the shortening direction (Z). However, orientation within the XY plane is dependent on the origin of the fabrics and the local strain state.

CONCLUSIONS

Pencil structure in the Knobs Formation of southwestern Virginia, U.S.A. is formed by intersection of bedding fissility and cleavage. The cleavage, defined by a mineral preferred orientation, results predominantly from pressure-solution associated with progressive bulk inhomogeneous shortening. Cleavage development is not due to brittle fracture, or shear, as implied by the term fracture cleavage. Straight chlorite fibres in pressure fringes around framboidal pyrites indicate that cleavage traces are parallel to the principal tectonic extension direction (X). Pencil development requires the presence of two independent fabric anisotropies, cleavage and bedding which are approximately equal in magnitude. This condition is met only within a certain range of strain values (9% shortening $\leq e_3 \leq$ 26% shortening). Where strains are less, cleavage is incipient and bedding fissility dominates. Where strains are higher, bedding fissility is destroyed and well developed cleavage dominates. Once the proper fabrics are present, stress relaxation attendant upon removal of confining pressures, results in strain-induced fractures parallel to the existing anisotropy directions. Therefore, within the same lithology, the transition from virtually undeformed bedding fissility, through pencils, and finally to cleavage represents a continuous fabric progression with increasing strain during deformation.

Pencil shape is specified by a shape factor ratio (l/w), where 'l' is pencil length and 'w' is pencil width measured in the bedding. Length and width of the fragments are dependent on the degree of anastomosing of cleavage traces on the bedding surface. Three-dimensional strain analysis (assuming no volume loss) using chlorite pressure fringes adjacent to framboidal pyrites, indicates that cleavage associated with pencil structure developed in plane strain. Also, pencil elongation is parallel to the intermediate axis of finite strain (Y). Moreover, the pencil shape factor is strain dependent and defined by the unique relation

$$l/w = 52.63\ (Y/Z) - 48.05.$$

With increasing strain, microfabric changes in the mudstone/siltstone produce pencils with higher length to width ratios. These changes include lengthening of cleavage traces, reduction in degree of anastomosing as cleavage traces tend towards planarity, and decrease in cleavage spacing.

Pencil structure in weakly deformed rock either develops due to intersection of independent fabric anisotropies (Cloos 1957, Crook 1964, Graham 1978, Engelder & Geiser 1979, this paper), or as a linear constrictional fabric (Ramsay 1981). Pencils produced by both mechanisms are potential strain markers. Derivation of a relation between pencil shape and strain provides another method for measuring deformation intensity. Regional strain patterns can be delineated, mechanisms of regional folding evaluated and the influence of faulting on fabric development determined in weakly deformed mudrock and siltstone.

Acknowledgements—The work was completed by I.J.R. as part of the requirements for an M.Sc. degree at Virginia Polytechnic Institute and State University. Academic year support was provided by a Departmental Graduate Teaching Assistant. Field support was from a Grant-in-Aid from Sigma Xi (the Scientific Research Society of North America) and a research grant from the Geological Society of America (donation from the Mobile Oil Corporation) all awarded to I.J.R. Summer support was from National Science Foundation Grant No. EAR 79-19703 awarded to D.R.G.

We thank J. F. Read, P. Geiser and A. W. Siddans for their comments on the manuscript. Assistance for paper preparation was given by V.P.I. & S.U.; thanks are extended to Martin Eiss and Sharon Chiang for drafting, Donna Williams for typing and Cynthia Zauner for photography.

REFERENCES

Bell, T. H. 1981, Foliation development — the contribution, geometry and significance of progressive, bulk, inhomogeneous shortening. *Tectonophysics* **76**, 273–296.

Cloos, E. 1957. Lineation, a critical review and annotated bibliography. *Mem. geol. Soc. Am.* **18**, 1–122.

Crook, K. A. W. 1964. Cleavage in weakly deformed mudstones. *Am. J. Sci.* **262**, 523–531.

Durney, D. W. & Ramsay, J. G. 1973. Incremental strains measured by syntectonic crystal growths. In: *Gravity and Tectonics* (edited by De Jong, D. A. & Scholten, R.) Wiley, New York, 67–96.

Engelder, T. & Sbar, M. L. 1977. The relationship between *in situ* strain relaxation and outcrop features in the Potsdam Sandstone, Alaxandra Bay, New York. *Pageoph.* **115**, 41–55.

Engelder, T. & Geiser, P. 1979. The relationship between pencil cleavage and lateral shortening within the Devonian section of the Appalachian Plateau, New York. *Geology* **7**, 460–464.

Epstein, A. G., Epstein, J. B. & Harris, L. D. 1976. Conodont color alteration—an index to organic metamorphism. *Prof. Pap. U.S. geol. Surv.* **995**, 1–27.
Friedman, M. 1972. Residual elastic strain in rocks. *Tectonophysics* **15**, 297–330.
Graham, R. H. 1978. Quantitative deformation studies in the Permian rocks of Alpes-Maritimes. Goguel Symposium, B.R.G.M., 220–238.
Gray, D. R. & Durney, D. W. 1979. Investigations on the mechanical significance of crenulation cleavage. *Tectonophysics* **58**, 35–79.
Holeywell, R. C. & Tullis, T. E. 1975. Mineral reorientation and slaty cleavage in the Martinsburg Formation, Lehigh Gap, Pennsylvania. *Bull. geol. Soc. Am.* **86**, 1296–1304.
Holzhausen, G. R. & Johnson, A. M. 1979. The concept of residual stress in rock. *Tectonophysics* **58**, 237–267.
Powell, C.McA. 1979. A morphological classification of rock cleavage. *Tectonophysics* **58**, 21–34.
Ramsay, J. G. 1981. Tectonics of the Helvetic Nappes. In: *Thrust and Nappe Tectonics* (edited by McClay, K. R. & Price, N. J.) *Spec. Publs geol. Soc. Lond.* **9**, 293–309.
Ramsay, J. G. & Wood, D. S. 1973. The geometric effects of volume change during deformation processes. *Tectonophysics* **16**, 263–277.
Reks, I. J. 1981. Strain, mesoscopic structure and cleavage in the Pulaski thrust sheet, southwestern Virginia. Unpublished M.Sc. Thesis, V.P.I. & S.U., Blacksburg, VA.
Sanderson, D. J. 1976. The superposition of compaction and plane strain. *Tectonophysics* **30**, 35–54.
Siddans, A. W. B. 1977. The development of slaty cleavage in a part of the French Alps. *Tectonophysics* **39**, 533–557.
Stringer, P. & Lajtai, E. Z. 1979. Cleavage in Triassic rocks of southern New Brunswick, Canada. *Can. J. Earth Sci.* **16**, 2165–2180.
Wickham, J. S. 1973. An estimate of strain increments in naturally deformed carbonate rock. *Am. J. Sci.* **273**, 23–47.
Wood, D. S. & Oertel, G. 1980. Deformation in the Cambrian Slate Belt of Wales. *J. Geol.* **88**, 285–308.

APPENDIX I

Sample locality	*UTM location	General location and lithology
53	4060250 m N 423870 m E	Roadcut at intersection of state route 772 and Russell Branch; blue–gray siltstones and mudstones
126	4059600 m N 412950 m E	Roadcut alongside state route 75, just south of Free Zion Church; blue–gray siltstones and mudstones
75	4061550 m N 422750 m E	Roadcut along Honey Locust Branch; green–gray siltstones.
21	4056050 m N 427330 m E	Roadcut along mountain road north of Vails Mill; black shales
122	4059270 m N 413240 m E	Roadcut along state route 75 near Blind Hollow; gray siltstones and sandstones
36(2)	4059100 m N 422520 m E	Roadcut along U.S. route 58 north of Osceola; blue–gray siltstones and mudstones
35	4059130 m N 422480 m E	Roadcut along U.S. route 58 north of Osceola; blue-gray siltstone and mudstones
253c	4074880 m N 451430 m E	Roadcut along interstate 81 west of Marion, VA; limy mudstone
158	4060340 m N 419290 m E	Roadcut along state route 75; blue–gray siltstones
17(2)	4057450 m N 427850 m E	Roadcut along state route 91, north of Wright Bridge; gray siltstones and mudstones
253 A	4074880 m N 451430 m E	Roadcut along interstate 81 west of Marion, VA; limy mudstone
253 B	4074880 m N 451430 m E	Roadcut along interstate 81 west of Marion, VA; limy mudstone
72	4061240 m N 422600 m E	Roadcut along Honey Locust Branch; blue–gray siltstone
54	4060800 m N 423840 m E	Roadcut along Russell Branch; gray–green siltstones and sandstones
57	4060430 m N 424280 m E	Roadcut along small road west of High Point school; brown–gray siltstones and sandstones
66	4060140 m N 422460 m E	Roadcut along Honey Locust Branch; tan–green siltstones

*UTM = Universal Transverse Mercator Grid.

APPENDIX II: PENCIL DATA

Sample locality	Sample size	L (mm)*	W (mm)*	L/W†	Distribution
53	37	97.42	4.35	23.09 ± 2.05	Linear
126	35	101.96	4.39	22.46 ± 2.10	Linear
75	53	99.76	4.72	21.11 ± 2.85	Linear
21	75	68.09	3.40	19.83 ± 3.07	Linear
122	75	99.51	5.28	19.77 ± 3.71	Linear
36(2)	50	86.03	4.49	19.19 ± 3.01	Linear
35	35	104.12	5.44	19.14 ± 2.07	Linear
253C	75	92.47	5.79	16.10 ± 2.92	Diffuse linear
158	100	63.27	4.11	15.57 ± 2.64	Linear
17(2)	50	76.11	5.78	13.42 ± 3.65	Diffuse linear
253A	100	23.42	1.83	13.15 ± 2.66	Point
253B	100	44.22	3.50	13.10 ± 3.29	Point
72	50	96.56	7.79	12.73 ± 3.95	Diffuse linear
54	36	115.41	9.88	11.72 ± 1.53	Linear
57	50	23.84	2.31	10.39 ± 1.55	Point
66	75	51.24	5.30	9.76 ± 1.10	Linear

* Mean values. † Mean ± standard deviation